

Calculation of High-pressure Argon Plasma Parameters Produced by Excimer Laser

TSUDA Norio and YAMADA Jun

Dept. of Electronics, Aichi Institute of Technology, Toyota-shi 470-0392, JAPAN

(Received: 18 January 2000 / Accepted: 12 May 2000)

Abstract

When a XeCl excimer laser light was focused in a high-pressure argon gas up to 150 atm, a dense plasma developed not only backward but also forward. It is important to study on the electron density and temperature of the laser-induced plasma in the high-pressure gas. The electron density and temperature in high-pressure argon plasma produced by XeCl excimer laser has been calculated and compared with the experimental data.

Keywords:

excimer laser, high-pressure plasma, electron density, electron temperature

1. Introduction

When an intense laser light is focused in a high-pressure gas, extremely dense plasma can be easily produced [1]. It is possible to use such plasma as a dense plasma source. The value of electron density of plasma produced in high-pressure gas above several thousand atm by focused laser light is equal to the obtainable value by using the solid target.

Various studies have been carried out on the mechanism of the gas breakdown [2], the interaction between the laser light and plasma [3], and the breakdown threshold [4]. The plasma produced by the visible laser developed only backward, because plasma frequency is higher than the laser one. But, an ultraviolet laser light can propagate through the plasma. The plasma develops not only backward but also forward [1]. The forward plasma development suddenly stops during the laser irradiation. The forward plasma radius is much smaller than the theoretical light cone [1]. The new forward development model, which includes the self-focusing effect and the absorption by the backward plasma, was proposed. This model could predict the development behavior reasonably well in all

stage.

It is important to study on the electron density and temperature of the laser-induced plasma in the high-pressure gas for understanding the development mechanism. But these have not been enough studied yet. The electron density and temperature in high-pressure argon plasma produced by XeCl excimer laser has been calculated and compared with the experimental data.

2. Plasma Property

The experimental setup is the same as in the previous article [1]. The XeCl excimer laser with a maximum power of 17 MW, a wavelength of 308 nm and a full half-width of 30 ns is focused. A lens with a focal length of 40 mm is used. As the laser light beam is a rectangle of 11 mm \times 24 mm, the focused laser beam at the focal spot makes an ellipse of 120 μ m \times 80 μ m. The pressure ranges from 1 to 150 atm.

A Typical plasma boundary observed by streak camera is shown in Fig. 1. The laser light is irradiated from the right, the time is scanned from top to bottom, the horizontal direction shows the plasma length, and

Corresponding author's e-mail: tsuda@el.aitech.ac.jp

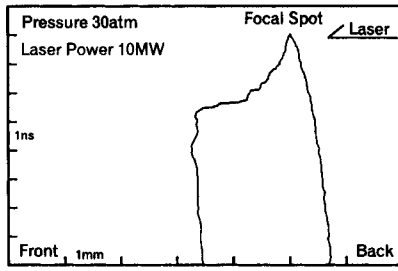


Fig. 1 Typical streak image of plasma boundary.

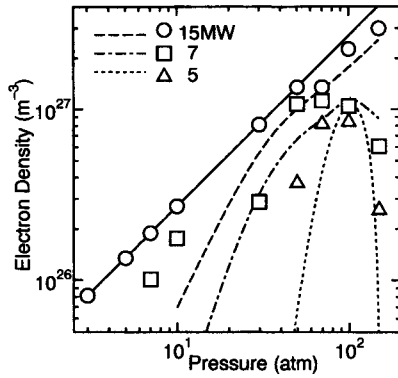


Fig. 2 Pressure dependence of electron density.

the inside of the boundary shows the plasma. After the plasma is produced at the focal spot, it simultaneously develops backward and forward. The forward plasma development velocity increases with increasing time, and after that the forward plasma stops developing even during the laser irradiation.

3. Electron Density

The peak electron density is measured by the Mach-Zehnder interferometer [5]. Pressure dependence of electron density is shown in Fig. 2. The electron density at the focal spot is proportional to the pressure and a fully ionized state is almost achieved up to 150 atm, when the laser intensity is 2×10^{11} W/cm². The electron density on the order of $10^{26} - 10^{27}$ m⁻³ is obtained.

The electron density is calculated by the simple rate equation, which takes into consideration of the collision ionization and the two-electron three-body recombination process.

The time variation of electron density depends on one of the laser pulse. Then, the waveform of laser pulse is expressed by the three polynomial functions [1]. Electron density is calculated using the observed

electron temperature. The calculated electron density is slightly lower than the experimental one at the low pressure below 30 atm, because measured electron temperature may be underestimated when the pressure is low.

4. Collisional and Radiative Processes in the Plasma

4.1.1 Ionization

The rate of ionization by collision of the electron with the neutral atom per unit volume and unit time is given as follows;

$$v_{egi} = N_g \int_{W_i}^{\infty} f_e(W_e) \sigma_{egi}(W_e) v_e dW_e, \quad (1)$$

where v_{egi} is the ionization frequency, N_g the density of neutral atom, $f_e(W_e)$ the electron energy distribution, v_e the electron thermal velocity, $\sigma_{egi}(W_e)$ the ionization cross section by the collision of the electron with the neutral atom, W_e the electron energy and W_i the ionization energy.

The cumulative ionization by the collision of the electron with excited atom is not considered in calculation because the cumulative ionization frequency is smaller than the collisional ionization frequency by the collision of the electron with the ground state atom.

4.1.2 Collision frequency of electron and ion

The collision frequency v_{ei} by elastic collision of electron and ion is given by

$$v_{ei} = 3.64 \times n_e T_e^{-\frac{3}{2}} \ln \left(\frac{1.25 \times 10^4 T_e^{\frac{3}{2}}}{n_e^{\frac{1}{2}}} \right). \quad (2)$$

Where n_e is the electron density and T_e the electron temperature.

4.1.3 Collision frequency of electron and neutral atom

The collision frequency v_{eg} by elastic collision of electron and neutral atom is given by

$$v_{eg} = 1.22 \times 10^{-14} N_g \int_0^{\infty} \frac{3kT_e}{2} dT_e. \quad (3)$$

4.2 Excitation probability

4.2.1 Averaged excitation probability and ionization probability

The averaged excitation probability qe and the ionization probability qi are shown in Fig. 3. Because the averaged excitation probability is lower than the ionization probability, the excitation probability is not considered in this calculation. The collisional ionization

frequency is obtained by fitting to the ionization probability.

4.3 Diffusion

The bipolar diffusion is dominant for radial direction in laser-induced high-pressure plasma, because the peak electron density at the focal spot is 10^{27} m^{-3} . The rate of diffusion loss is given by

$$\frac{n_e}{\tau} = \left(\frac{2.4}{r}\right)^2 \frac{\mu_i k T_e}{e} n_e, \quad (4)$$

where τ is the diffusion time, r the average radius of laser-induced plasma, and μ_i the mobility of the ions.

4.4 Coefficient of thermal conductivity

Thermal conductivity coefficient κ , translation energy κ_e^{tr} and reaction energy κ_{reac} are shown in Fig. 4. The coefficient of thermal conductivity is divided into four sections. The thermal conductivity is expressed by four polynomial functions.

5. Electron Temperature

The electron temperature is calculated from energy balance equation, which takes into consideration of the gain by the inverse bremsstrahlung and the loss by the collisional ionization of electron, the elastic collision, the heat conduction and the diffusion.

$$\begin{aligned} \frac{\partial T_e}{\partial t} = & \frac{2}{3k} N_g \sigma_{en} \frac{W(t)}{\pi r_{\parallel} r_{\perp}} - \frac{2m}{M} T_e (v_{eg} + v_{ei}) \\ & - \frac{2}{3k} v_{egi} W_i - \kappa \frac{2}{3k} \frac{\partial T_e}{\partial x} \frac{1}{n_e} \\ & - \frac{2}{3} \left(\frac{2.4}{r}\right)^2 \frac{\mu_i}{e} W_i, \end{aligned} \quad (5)$$

where σ_{en} is the cross section for absorption of the photon, $W(t)$ is the laser power, r_{\parallel} and r_{\perp} are the horizontal and the vertical radius at the focal spot, m is the electron mass, M is the atom mass.

Temporal variation of measured and calculated electron temperatures are shown in Figs. 5 and 6. In the temporal variation of measured electron temperature, the peak time of electron temperature is nearly equal to the end of the laser pulse at low pressure. However, it becomes faster with increasing pressure, and it equals the peak time of laser pulse, because the energy loss due to thermal conduction is large.

The temporal variation of calculated electron temperature qualitatively agrees with the measured one.

However, the peak electron temperature is one order higher than the measured value, because the electron temperature is calculated using the value of the approximate thermal conduction coefficient obtained by

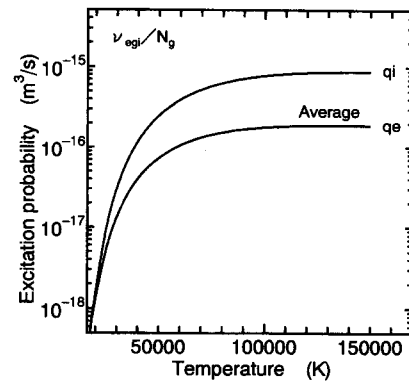


Fig. 3 Averaged excitation probability and ionization probability.

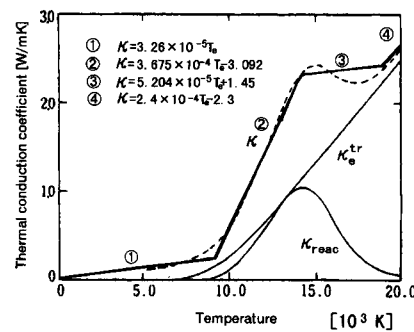


Fig. 4 Thermal conduction coefficient.

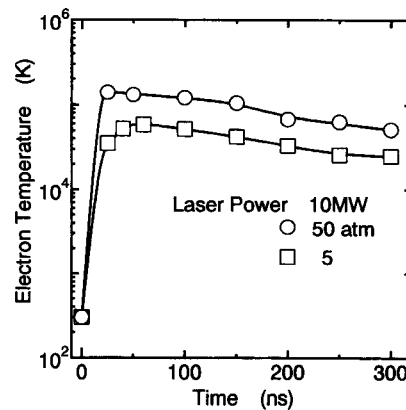


Fig. 5 Time variation of measured electron temperature.

extrapolating above 20000 K.

Pressure dependence of measured and calculated electron temperatures are shown in Figs. 7 and 8. The broken lines indicate electron temperatures estimated from spectral line intensity ratio of several argon II lines, and solid lines show those estimated from

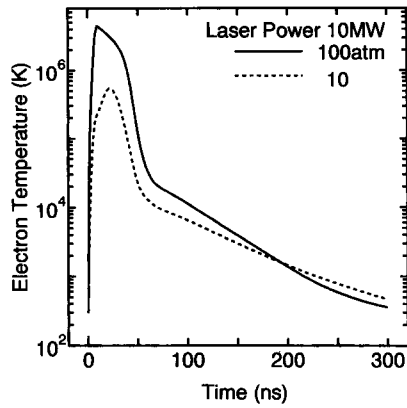


Fig. 6 Time variation of calculated electron temperature.

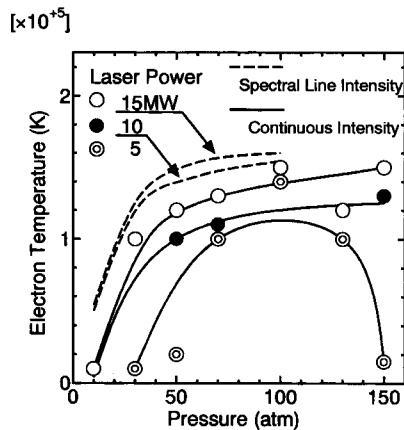


Fig. 7 Pressure dependence of measured electron temperature.

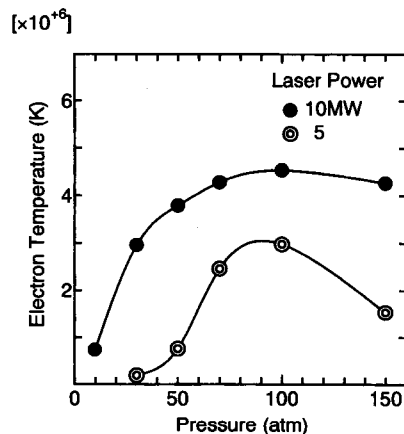


Fig. 8 Pressure dependence of calculated electron temperature.

continuous intensity.

Electron temperature of the order of 10^5 K is obtained at the focal spot [6]. Electron temperature increases with increasing pressure, but it saturates above 50 atm, and decreases above 100 atm when the laser power is lower.

In pressure dependence of calculated electron temperature, the calculated electron temperature qualitatively agrees with the measured one.

6. Conclusion

The electron density and temperature has been theoretically calculated and compared with the experimental data.

Calculated electron density agrees with the measured value, and the electron density reaches 10^{27} m^{-3} when the pressure is 150 atm and laser power is 15 MW.

The calculated electron temperature is in qualitative agreement with the measured value. However, it is one order higher than the measured value, because thermal conduction coefficient has not been measured above 20000 K, and the electron temperature is calculated using the value obtained by extrapolating.

References

- [1] N. Tsuda *et al.*, *J. Appl. Phys.* **81**, 582 (1997).
- [2] R.G. Meyerand *et al.*, *Phys. Rev. Lett.* **11**, 401 (1963).
- [3] G.V. Ostrovskaya *et al.*, *Sov. Phys. Usp.* **16**, 834 (1974).
- [4] Yu. P. Raizer *Sov. Phys. JETP* **21**, 1009 (1965).
- [5] N. Tsuda *et al.*, *Jpn. J. Appl. Phys.* **36**, 4690 (1997).
- [6] N. Tsuda *et al.*, *Jpn. J. Appl. Phys.* **38**, 3712 (1999).